GEOPHYSICS, VOL. 77, NO. 4 (JULY-AUGUST 2012); P. V133–V142, 4 FIGS.
10.1190/GEO2011-0500.1

Bandwidth enhancement: Inverse Q filtering or time-varying Wiener deconvolution?

Mirko van der Baan[1]

ABSTRACT

Dispersion and attenuation corrections can improve the resolution of seismic data. This significantly facilitates interpretation. In principle, inverse Q filtering and the time-varying Wiener deconvolution can achieve this. Inverse Q filtering is a deterministic process that requires knowledge of the quality factor Q, whereas the time-varying Wiener deconvolution is a statistical approach based on the estimation of the nonstationary propagating wavelet. Dispersion corrections based on phase-only inverse Q filtering is an inherently stable method that is robust in the presence of noise. Attenuation corrections via amplitude-only inverse Q filtering, on the other hand, is likely to lead to noise amplification as well as bandwidth enhancement. Dispersion corrections via the time-varying Wiener deconvolution are challenging because these require estimation of a nonstationary, frequency-dependent, nonminimum-phase wavelet. Fortunately, attenuation corrections via the Wiener deconvolution need only estimation of a zero-phase time-varying wavelet for which robust methods exist. The most promising procedure for combined dispersion and attenuation correction is thus comprised of first applying dispersion corrections using phase-only inverse Q filtering, followed by zero-phase time-varying Wiener deconvolution.

INTRODUCTION

There has been renewed interest in inverse Q-based attenuation corrections either before or even during prestack migration (Ferber, 2005; Mittet, 2007; Birdus and Artyomov, 2011; Cavalca et al., 2011). Such corrections are important because they offer the promise of creating the highest possible resolution by expanding the range of the local frequency content. The greatest challenge lies in developing algorithms that are robust in addition to correctly estimating the appropriate quality factor Q.

Even though attenuation corrections are challenging, attenuation and dispersion are concomitant. Dispersion corrections based on phase-only inverse Q filtering are therefore routinely applied to most data sets. This is an inherently stable process because no energy is boosted, but it solely involves phase changes (Robinson, 1979).

Dispersion corrections already improve resolution by rendering recorded waveforms to zero phase and thus more symmetric. This assumes the near-surface wavelet is already zero-phase or has been made zero phase. The near-surface wavelet is defined as the source wavelet convolved with all near-surface effects, including instrument response, ground coupling, the effects of weathering layers, etc. Both surface-consistent deconvolution in land processing and debubbling corrections in marine processing are aimed at collapsing this wavelet (van der Baan et al., 2010). Symmetric waveforms have higher resolution than asymmetric ones because they concentrate most energy close to their center, thus allowing for more closely spaced reflections to be more readily visible in seismic data (Schoenberger, 1974). A second advantage of dispersion corrections is that they facilitate seismic-to-well ties by creating a more stationary wavelet (Ziolkowski et al., 1998).

The current renewed interest in robust attenuation corrections originates in the continued need for enhanced resolution to detect and appraise increasingly more subtle reservoirs. Many acquisition and processing strategies favor corrections based on deterministic laws instead of statistical principles (Trantham, 1994) because the former are predictable and repeatable. Unfortunately, repeatability does not guarantee reversibility. Attenuation corrections based on inverse Q filtering are founded on deterministic processes; yet they are not necessarily stable because energy amplification is involved. In this paper, I will contrast and compare attenuation and dispersion corrections based on inverse Q filtering and time-varying Wiener deconvolution. The latter is an example of a statistical method. Differences and similarities between the time-varying Wiener

Manuscript received by the Editor 9 December 2011; revised manuscript received 18 March 2012; published online 22 June 2012.
[1]University of Alberta, Deptartment of Physics, Edmonton, Alberta, Canada. E-mail: Mirko.vanderBaan@ualberta.ca.

deconvolution and the Gabor deconvolution (Margrave et al., 2011), another statistical method, are also discussed.

First, I describe the mathematical principles on which all techniques are based. I then introduce a new implementation for inverse Q-based attenuation corrections. Finally, I compare the advantages and inconveniences of inverse Q filtering and time-varying Wiener deconvolution on synthetic and real data examples.

THEORY

Inverse Q filtering

The time-domain response $u(t,z)$ of a pulse that has propagated to a depth z can be written as the superposition of monochromatic waves in the frequency domain as

$$u(t,z) = \int S_0(\omega) \exp\{i(kz - \omega t)\} d\omega, \tag{1}$$

where u is displacement, t is time, z is depth, S_0 represents the original source signal, k is a complex-valued wavenumber, and ω is angular frequency (Futterman, 1962). For simplicity, I set $S_0 = 1$. Hence, the initial source signal is a unit pulse. Its actual shape has little relevance for the proposed method.

In an elastic medium the vertical wavenumber k will be real valued; yet in general it is complex valued because attenuation occurs in most, if not all, materials. A common strategy is to express wavenumber k as the multiplication of a real-valued part k_r and a portion related to the quality factor Q via (Bickel and Natarajan, 1985)

$$k = k_r \left(1 + \frac{i}{2Q}\right). \tag{2}$$

The sign of the imaginary part in this equation depends on the sign convention used for the temporal Fourier transform in expression 1.

Attenuation and dispersion are concomitant. It thus remains to specify an appropriate dispersion relation. Two commonly used ones are, respectively, by Futterman (1962) and Kjartansson (1979), given by

$$k_{r,\text{Futt}} = \frac{\omega}{c_0}\left[1 - \frac{1}{\pi Q} \ln\left(\frac{\omega}{\omega_0}\right)\right], \tag{3}$$

and

$$k_{r,\text{Kjar}} = \frac{\omega}{c_0}\left(\frac{\omega}{\omega_0}\right)^{-\frac{1}{\pi Q}}, \tag{4}$$

with c_0 the phase velocity associated with reference frequency ω_0.

Substitution of equation 2 into expression 1 in combination with the appropriate dispersion relationship 3 or 4 then describes the propagation of a pulse in an attenuative medium. Defining $t_0 = z/c_0$ as the arrival time of this pulse at reference frequency ω_0, one obtains

$$u(t,t_0) = \int \exp\{i\omega(t_0\gamma - t)\} \exp\left\{-\frac{\omega t_0 \gamma}{2Q}\right\} d\omega, \tag{5}$$

where γ can be interpreted as a dimensionless frequency-dependent slowness defined by the chosen dispersion law. For completeness it is given by

$$\gamma_{\text{Futt}} = \left[1 - \frac{1}{\pi Q} \ln \frac{\omega}{\omega_0}\right], \tag{6}$$

for the Futterman dispersion law, equation 3, and

$$\gamma_{\text{Kjar}} = \left(\frac{\omega}{\omega_0}\right)^{-\frac{1}{\pi Q}}, \tag{7}$$

for the Kjartansson dispersion law, equation 4.

Equation 5 is conveniently computed using an inverse Fourier transform, FT^{-1}. For instance, to obtain the seismogram for a spike traveling from $t = 0$ to $t = t_0$, one computes

$$u(t,t_0) = FT^{-1}\left[\exp\{i\omega t_0\gamma\} \exp\left\{-\frac{\omega t_0 \gamma}{2Q}\right\}\right]. \tag{8}$$

The first exponent in equation 8 describes all dispersion effects, the second exponent describes all amplitude attenuation.

Equations 5 and 8 are the basis for the dispersion correction of Robinson (1979) and Hargreaves and Calvert (1991) as well as the inverse Q filtering techniques of Bickel and Natarajan (1985), Hargreaves and Calvert (1991) and Wang (2002) to correct for dispersion and attenuation. Specifically, Hargreaves and Calvert (1991) note that equations such as expression 5 can be reformulated into a migration algorithm based on wavefield extrapolation by linking the wavefield $u(t,t_0)$ at time t_0 to the wavefield $u(t,t_0+\Delta t)$ at a time step Δt earlier or later. Thus, from equations 5 and 8,

$$\begin{aligned} u(t,t_0+\Delta t) &= FT^{-1}\left[\exp\{i\omega(t_0+\Delta t)\gamma\} \exp\left\{-\frac{\omega(t_0+\Delta t)\gamma}{2Q}\right\}\right] \\ &= FT^{-1}\left[FT[u(t,t_0)] \exp\{i\omega\Delta t\gamma\} \exp\left\{-\frac{\omega\Delta t\gamma}{2Q}\right\}\right], \end{aligned} \tag{9}$$

with FT the forward Fourier transform and FT^{-1} its inverse.

Equation 8 describes the propagation of a spike from the origin to two-way traveltime t_0. Expression 9 can thus be interpreted as a generalization of formula 8 because it propagates the source wavefield $u(t,t_0)$ to that a time step Δt earlier or later.

Expression 9 is very flexible in that forward propagation is achieved using positive time steps Δt and reverse propagation using negative steps. Inverse Q dispersion and attenuation corrections are thus in principle feasible by employing negative time steps Δt on a recorded seismogram. Note that the first exponent affects solely the phase and is thus entirely related to dispersion; conversely, the second exponent influences solely the amplitudes and thereby attenuation. Phase corrections are inherently stable irrespective of the sign of time step Δt and the magnitude of the quality factor Q because no energy is amplified or dissipated. On the other hand, attenuation corrections using negative time steps Δt are always unstable because energy is boosted without an upper bound.

Equation 9 can be implemented in a variety of ways for combined amplitude-and-phase inverse Q filtering (e.g., Bickel and Natarajan, 1985; Hargreaves and Calvert, 1991; Wang, 2002) or even further simplified if only dispersion corrections are required.

Given an observed seismogram $u(t, t_0)$, equation 9 can be used to correct for the dispersion and some attenuation by back-propagating the arrival around time t_0 to the origin; in other words, by setting $\Delta t = -t_0$. Generally, in wavefield extrapolation, we are only interested in the part that has been migrated back to the origin, that is, to $t = 0$ as this is the imaging condition. Therefore, equation 9 is generally formulated as an integral over frequency instead of an inverse Fourier transform (Hargreaves and Calvert, 1991; Wang, 2002). Combining this with $\Delta t = -t_0$ produces

$$u(t = 0, t_0 + \Delta t = 0) = \frac{1}{2\pi} \int FT[u(t, t_0)] \exp\{-i\omega t_0 \gamma\} \exp\left\{\frac{\omega t_0 \gamma}{2Q}\right\} d\omega. \tag{10}$$

This expression can be solved by stepping over every possible arrival time t_0 with sampling interval Δt. The quantity $FT[u(t, t_0)]$ represents the Fourier transform of the entire observed trace because the wave equation is linear, resulting into linear superposition of all arrivals. The physical interpretation of expression 10 is that all plane-wave components in the observed signal are migrated back to the origin after dispersion and attenuation corrections.

Expression 10 can be simplified further if only dispersion corrections are desired by removing the second exponent and applying a change of variables given by $\omega' = \omega\gamma$ such that a single inverse Fourier transform instead of a loop over all arrival times t_0 produces the desired phase-only inverse Q compensated signal. See Robinson (1979), Hargreaves and Calvert (1991), and Wang (2002) for details.

Besides implementation nuances, the main differences for inverse Q filtering occur in the stability conditions used to prevent excessive noise amplification during any attenuation corrections. In this paper, I introduce a new implementation via a series of short-term Fourier transforms as well as a very simple user-set stability condition, namely, the second exponent in equation 9 is not allowed to exceed a maximum $c_{\max}$. Thus,

$$\exp\left\{-\frac{\omega \Delta t \gamma}{2Q}\right\} \le c_{\max}. \tag{11}$$

This ensures that no frequency components can be magnified beyond a user-set level. For convenience, dispersion corrections are implemented here by excluding the second exponent entirely.

I use equation 9 directly to correct for the dispersion and some attenuation by back-propagating the arrival around time t_0 to the origin. This procedure can be implemented using a loop over every recorded time sample by Fourier transforming either the entire seismogram or solely a relevant portion. Obviously, the latter approach involves less samples and is thus faster. The appropriate window length is determined by the spread in encountered dispersion for a negative back-propagation time step Δt and the length of the anticipated propagating wavelet (see van der Baan et al. [2010] for wavelet terminology).

An initial spiky pulse with infinite bandwidth arriving at reference time t_0 is spread out between the highest (fastest) and lowest (slowest) recorded frequency (excluding zero), respectively. The minimum start and end times are thus, respectively, $(1 - \gamma(\omega_{\max}))t_0$ and $(1 - \gamma(\omega_{\min}))t_0$, where equations 6 and 7 stipulate the relative dispersion γ given the appropriate dispersion law. However, in reality, all source signals and thus, propagating wavelets, have a limited bandwidth and are spread out in time. It is therefore recommended to expand the sides of the computed time window by, respectively, $-3/4$ and one times the length of the propagating wavelet l_w. The start t_s and end t_e times of the sliding window thus become

$$t_s = (1 - \gamma(\omega_{\max}))t_0 - 0.75 l_w, \tag{12}$$

and

$$t_e = (1 - \gamma(\omega_{\min}))t_0 + l_w. \tag{13}$$

The described approach leads to window lengths that are approximately proportional to the imaginary reference arrival at t_0 but will rarely include the origin time. At first sight, the extracted window might seem too short for back-propagation of the reference arrival to the origin. However, the frequency-domain implementation leads to circular convolution and thereby wrap around of energy within each time window. Appropriate tapering of both window edges prevents introduction of wrap-around artifacts. In practice, a taper length of $1/4$ or $1/3$ of the length of the propagating wavelet was found to be sufficient.

Equation 9 can then be used for pure dispersion corrections by excluding the second exponent as well as combined dispersion and partial attenuation corrections by back-propagation of energy. The threshold $c_{\max}$ (equation 11) prevents unlimited energy reconstruction.

The advantage of equation 9 is that no knowledge is required of the propagating wavelet at any stage except for a rough estimate of its length for tapering purposes. On the other hand, a sufficiently accurate estimate of the quality factor Q is needed. This topic will be addressed more adequately in the "Discussion" section.

A second disadvantage is that equation 9 implicitly assumes that all recorded data $u(t, t_0)$ are pure signal; that is, no mechanism is included to distinguish between noise and signal. This may lead to overall noise amplification, in particular, after attenuation corrections; the signal-to-noise ratio (S/N) at individual frequencies is maintained but specifically high-frequency noise may dominate the final result.

In the next subsection, I describe an alternative approach that explicitly differentiates between noise and signal, thus promising a mathematically optimal trade-off between signal enhancement and noise amplification.

Time-varying Wiener deconvolution

In the deconvolution problem, we assume that the observed trace x is the result of the convolution of the propagating wavelet w with the reflectivity series r plus some superposed noise n. That is,

$$x(t) = w(t) \star r(t) + n(t), \tag{14}$$

where $\star$ indicates convolution and t represents time. The propagating wavelet is the physical wavelet that propagates through the earth, thereby sampling the geology. This wavelet is subject to geometric spreading, apparent and intrinsic attenuation (e.g., due to stratigraphic filtering and multiple scattering) and concomitant

dispersion. Both seismic-to-well ties and studies of local attenuation aim to retrieve this wavelet (van der Baan et al., 2010).

The deconvolution objective is to find a filter $g(t)$ such that the outcome $y(t)$ is as close as possible to the original reflectivity series $r(t)$. Thus, $y(t) = g(t) \star x(t) \approx r(t)$. Because of the presence of the noise, the reflectivity series r cannot be recovered perfectly, and a compromise must be achieved between noise amplification and successful recovery.

If the wavelet $w(t)$ is known, then the time-domain Wiener filter $g_w(t)$ achieves an optimum solution in a least-squares sense. In the frequency domain, it is given by

$$G_w(f) = \frac{W^*(f)}{|W(f)|^2 + \sigma_n^2}, \tag{15}$$

with f frequency, σ_n^2 the noise variance, and superscript $*$ the complex conjugate (Berkhout, 1977). Capital letters denote the frequency-domain equivalent of a time-domain function. For instance, W is the frequency-domain expression of wavelet $w(t)$.

The Wiener deconvolution incorporates an explicit trade-off between recovery of the reflectivity series and noise amplification. In the wavelet passband, $|W|$ will be large with respect to the noise variance σ_n^2, such that $G_w \approx 1/W$. The Wiener filter is then close to the inverse of the wavelet filter yielding $y = g_w \star w \star r \approx r$, equation 14. On the other hand, at frequencies where the noise dominates, we have $G_w \approx W^*/\sigma_n^2 \approx 0$ such that all noise is strongly attenuated in this region. The Wiener filter therefore only whitens the observed signal within its passband.

Equation 15 assumes the propagating wavelet is stationary; yet the preceding discussion remains valid for nonstationary wavelets if combined with the time-varying Wiener deconvolution. The advantage of the time-varying Wiener deconvolution over inverse Q filtering is thus that the former explicitly discriminates between signal and noise. The disadvantage is that the amplitude and phase spectrum of a changing propagating wavelet must be known. Attenuation and dispersion corrections are thus feasible using the time-varying Wiener deconvolution if the propagating wavelet is known at each point in time and space. Suitable implementations are described in Clarke (1968), Wang (1969), and van der Baan (2008).

In this paper, I use the method of van der Baan (2008) to estimate and deconvolve a time-varying constant-phase wavelet. Estimation is achieved by kurtosis maximization and spectral averaging using extracted time segments. Dispersion corrections are by definition frequency dependent. The extracted wavelets are thus less suited for dispersion corrections. Unfortunately, to the best of my knowledge, no robust methods exist for nonstationary, frequency-dependent, nonminimum-phase wavelet estimation.

RESULTS

Synthetic examples

First, I illustrate some of the advantages and inconveniences of inverse Q filtering on a simple synthetic example. Figure 1a shows three reflections occurring at, respectively 0.5, 1.0, and 1.5 s, obtained using equation 8. The quality factor Q is 30. Futterman's dispersion law is employed (equation 6) with a reference frequency $f_0 = \omega_0/(2\pi)$ arbitrarily set to 20 Hz to be within the range of most seismic data. Both dispersion laws give comparable results unless very low values of Q are employed.

The initial shape of the propagating wavelet is a unit pulse. All variations in shape are due to attenuation and concomitant dispersion. Attenuation is demonstrated, for instance, by the reduction in maximum amplitude and reduction in rise time; that is, the initial slope of each arrival flattens with time. The dispersion is evidenced by the widening of the pulse and its increasing asymmetry with time because the lower frequencies arrive after the high-frequency components.

Figure 1b shows an undamped amplitude (attenuation) and phase (dispersion) inverse Q filtering using the correct quality factor of 30. This result is obtained by using a loop over all possible arrival times t_0 and extracting a local window defined by expressions 12 and 13. This window then represents $u(t, t0)$ in expression 9 with $\Delta t = -t_0$. The sample of the resulting seismogram $u(t, 0)$ at time zero yields the deconvolved outcome. In practice, a portion is extracted such that not every possible arrival time t_0 must be evaluated to increase computation speed. Futterman's dispersion law is again used (equation 6). For numerical stability, the wavelet length l_w is set to 150 ms in equations 12 and 13.

In an ideal world, Figure 1b would show three unit spikes at times 0.5, 1.0, and 1.5 s. Unfortunately, even in this noise-free example, unlimited signal reconstruction is not feasible due to finite numerical precision, thus explaining the resulting artifacts. Inverse Q filtering for attenuation correction is not unconditionally stable.

In Figure 1c, the procedure is repeated for phase-only inverse Q filtering to correct for all dispersion effects. Again, equation 9 is employed, but the second exponent related purely to attenuation is set to one. The resulting waveforms are symmetric indicating that all dispersion has been removed. Phase-only inverse Q filtering is therefore unconditionally stable.

Figure 1d then displays the result of a combined amplitude and phase inverse Q filtering. The difference with Figure 1b is that an upper limit is set for amplitude reconstruction using $c_{\max} = 100$ (equation 11). The dispersion correction is unconstrained. A damped attenuation correction can improve resolution by enhancing the bandwidth (Hargreaves and Calvert, 1991; Wang, 2002). This is visible in Figure 1d in the reduced width of the reconstructed wavelets compared with their original ones (Figure 1a). Later arrivals are less well reconstructed because more energy over a larger frequency range has attenuated beyond the recovery limit.

Next, the time-varying Wiener deconvolution is tested to remove attenuation and dispersion. The time-varying Wiener implementation is described in van der Baan (2008). Contrary to the inverse Q results where the exact value of Q is provided, the required wavelets are estimated. This is achieved by dividing the trace into seven segments with a 67% overlap and assuming the wavelet has a length of 200 ms, followed by spectral averaging (van der Baan, 2008).

The time-varying Wiener deconvolution using constant-phase wavelets does improve the bandwidth but is unable to correct for all dispersion (Figure 1e). The resulting deconvolved sections have compacted wavelets, but they are not zero phase. The inability to correct for the dispersion results from the use of constant-phase wavelets; dispersion is by its very nature a frequency dependent effect.

Finally, Figure 1f shows the effect of the time-varying Wiener deconvolution, applied after dispersion corrections obtained using phase-only inverse Q filtering (Figure 1c). The resulting filtered trace is very comparable with the one obtained using damped inverse Q filtering (Figure 1d). A higher value of threshold $c_{\max}$ in expression 11 could have recovered more signal in Figure 1d

because this is a noiseless example where the recovery limit is determined by the machine precision.

Next, the same synthetic example is considered with three reflections, but a small amount of noise is added (Figure 2a). A dispersion correction by phase-only inverse Q filtering using the correct quality factor continues to perform well because no noise amplification occurs (Figure 2b). A damped amplitude-and-phase inverse Q filtering, however, boosts the overall noise levels significantly, even if a lower threshold $c_{\max}$ of 20 is employed (Figure 2c). Application of the time-varying Wiener deconvolution applied after dispersion correction (Figure 2b) using estimated wavelets obtained using identical parameters as before produces comparable or possibly slightly better bandwidth enhancements but without noise amplification (Figure 2d). The preferred combination is thus, first a dispersion correction using phase-only inverse Q filtering, followed by the time-varying Wiener deconvolution for partial recovery of attenuated frequencies.

Real data examples

In the following, I consider two real data examples. The first is a marine data set known to have phase variations with two-way traveltime (van der Baan, 2008). Estimated wavelets are characterized by $-80°$ constant-phase rotations in the top 1 s, followed by $-40°$ between 1.5 and 3 s, and $-20°$ for times larger than 3 s (Figure 5 in van der Baan, 2008). Standard predictive deconvolution is applied to this data set but no dispersion or zero-phase corrections. The cause of the detected phase rotations is unknown but one possible explanation is that the initial near-surface wavelet is characterized by a 90° phase rotation and that all subsequent rotations are due to dispersion. Unfortunately, this does not explain the encountered staircase-like behavior in the estimated wavelet phase.

Figure 3a shows a zoomed in portion of the original data set, and Figure 3b shows the corresponding result after combined attenuation-and-dispersion corrections using amplitude-and-phase inverse Q filtering. A quality factor of 150 is used to enforce conservative corrections. Duren and Trantham (1997) argue that quality factors between 67 and 150% of the true value yield adequate dispersion corrections. This amounts to values of Q between 100 and 225 in this case. Threshold $c_{\max} = 5$ (equation 11) to prevent significant high-frequency noise amplification throughout the data set, especially in the deeper portions (not shown). Again, a wavelet length of 150 ms is assumed.

Full inverse Q filtering has shortened the reflections at 2.35 and 2.5 s and thus improved their resolution. This occurs, however, at the expense of the reflectors underneath. For instance, the reflector at 2.78 s stands out barely above the overall noise level contrary to in the original data (Figure 3a). This undesired effect is even more pronounced for lower reflectors.

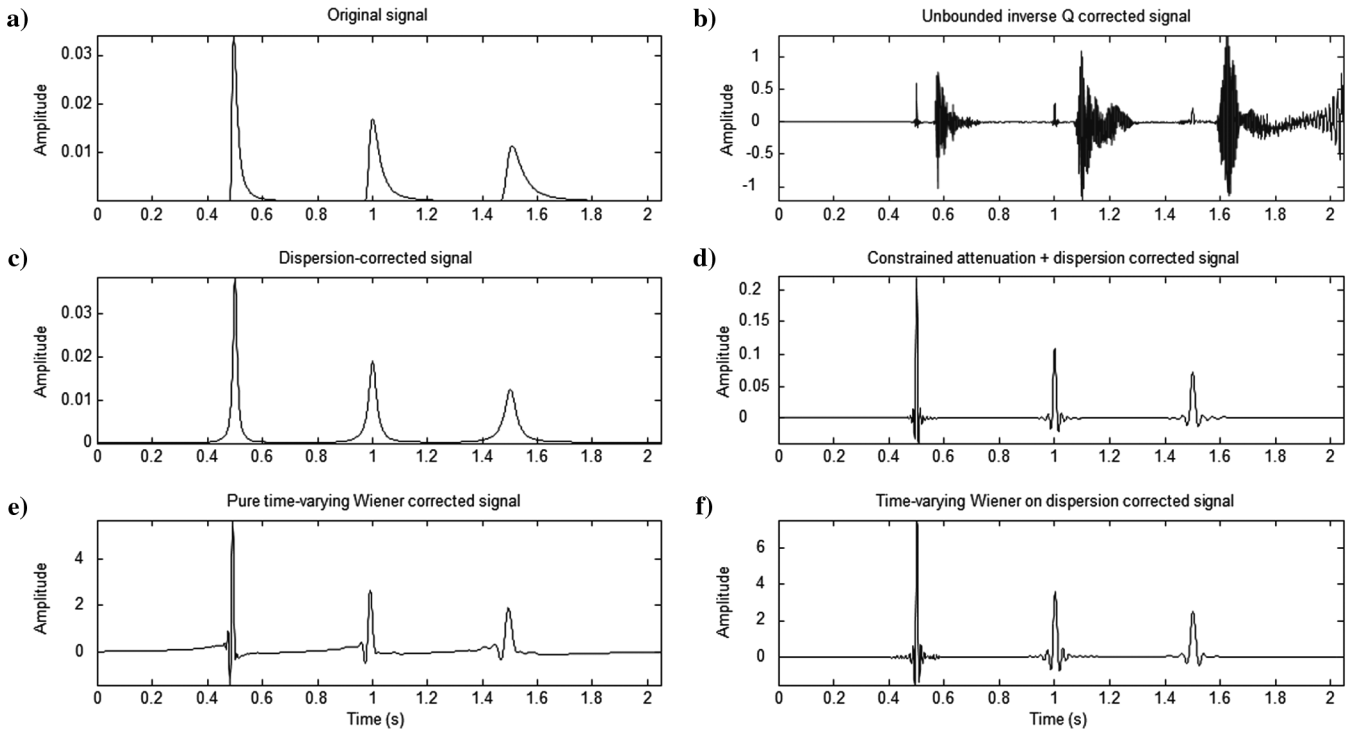

Figure 1. Attenuation and dispersion corrections on a noiseless synthetic example. (a) Original trace containing three reflections at 0.5, 1.0, and 1.5 s. The initial wavelet is a spike and the quality factor is 30. (b) Unconstrained inverse Q filtering leads to unbounded amplification of amplitudes and the creation of many undesired artifacts even in a noiseless data example. (c) Dispersion corrections using phase-only inverse Q filtering is unconditionally stable and reconstructs symmetric zero-phase wavelets. (d) Constrained amplitude-and-phase inverse Q filtering limits the reconstruction of energy thus enhancing bandwidth and resolution. (e) Time-varying Wiener deconvolution using constant-phase wavelets cannot correct for dispersion because this is by definition a frequency-dependent process, although bandwidth has been improved. (f) Zero-phase time-varying Wiener deconvolution applied after phase-only inverse Q filtering leads here to similar results as constrained amplitude-and-phase inverse Q filtering.

A dispersion correction using phase-only inverse Q filtering does not raise noise levels, yet produces more symmetric waveforms (Figure 3c). Subsequent time-varying Wiener deconvolution (Figure 3d) then enhances the resolution by expanding the recorded signal bandwidth within the limits of the passband of the propagating wavelet. For instance, a single reflection is visible in the original data around 2.5 s (Figure 3a), yet in the final image, there is evidence for two reflections (Figure 3d).

The second data set is from the Williston Basin in Saskatchewan, Canada. It is also analyzed in van der Baan et al. (2010). Figure 4a zooms in on one of the Devonian reefs (visible at 1.4 s and common depth points 220–240). No dispersion corrections are applied to the original data set, but it has been subjected to predictive deconvolution as well as time-varying spectral balancing.

A full inverse Q filtering enhances resolution but blankets many reflections by raising the overall noise level to a constant energy level (Figure 4b). Identical parameters as for the previous real-data example are used.

A dispersion correction renders most waveforms again more symmetric and thus zero phase (Figure 4c). A subsequent time-varying Wiener deconvolution emphasizes the major reflections even more, possibly at the expense of some of the smallest ones (Figure 4d).

DISCUSSION

Many acquisition and processing strategies favor corrections based on deterministic laws due to their predictability and repeatability (Trantham, 1994). Inverse-Q filtering is such a deterministic process; yet repeatability does not guarantee reversibility. Most amplitude inverse-Q implementations are based on equation 10 or similar variants (Hargreaves and Calvert, 1991; Wang, 2002). They also use somewhat different damping strategies and numerical implementations to limit the total gain and speed up the computations than described here. Bickel and Natarajan (1985) and Wang (2002) use a specific constraint on the included upper frequency, namely, the maximum frequency is proportional to $2Q/t_0$. Wang (2002) combines this with a threshold similar to equation 11. Wang (2006) uses an alternative criterion that has the advantage that it is partially reversible, making parameter testing convenient.

Differences in the various numerical implementations are not likely to change the final inverse Q results significantly, but they do impact computation times. Direct implementation of expression 10 involves one forward Fourier transform and an integration repeated for every time sample. This leads to a computational cost proportional to $n \log n + n^2$ with n the number of time samples. I assume here the cost of an integration is n and that of a Fourier

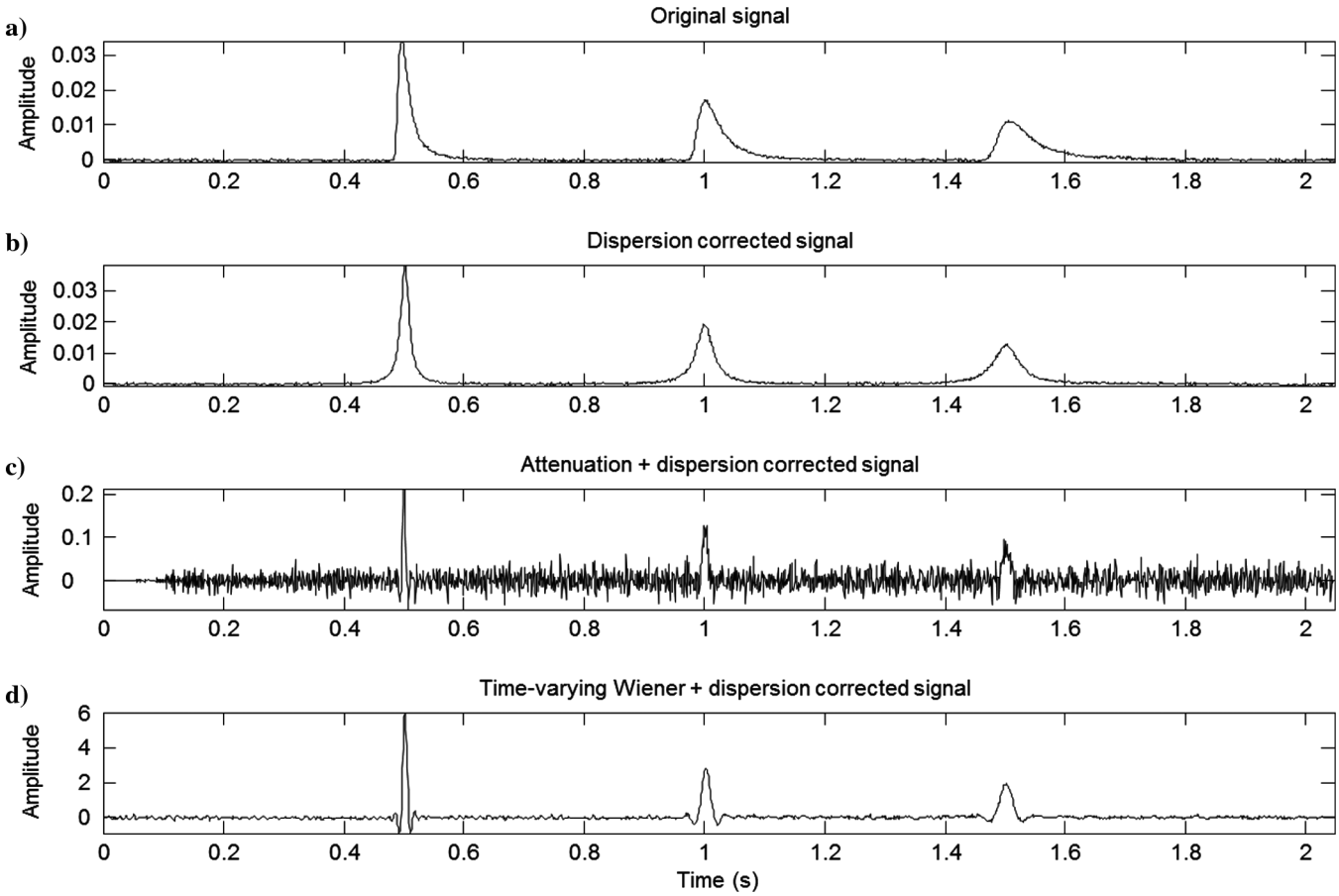

Figure 2. Attenuation and dispersion corrections on a noisy synthetic example. (a) The same synthetic example as in Figure 1a is used but with added noise. (b) Dispersion corrections using phase-only inverse Q filtering reconstructs again symmetric zero-phase wavelets without noise amplification. (c) Constrained amplitude-and-phase inverse Q filtering boosts resolution but at the expense of significant high-frequency noise amplification. (d) Zero-phase time-varying Wiener deconvolution applied after phase-only inverse Q filtering boosts again the bandwidth and resolution but without significant noise amplification.

transform $n \log n$. Implementation of equation 9 using the entire trace is more expensive because it involves a forward Fourier transform and an inverse transform repeated n times, yielding a cost proportional to $n \log n + n^2 \log n$. The use of a short-time Fourier transform with a fixed length n/m and step size $k\Delta t$ has an approximate cost of $\frac{2n^2}{mk} \log(n/m)$ that is already faster than direct use of imaging equation 10 for $\frac{\log(n/m)}{mk} > 1/2$. Wang (2002) may offer a more cost-efficient implementation than described here by using piecewise approximations for the second exponent in imaging expression 10 followed by a forward and inverse Fourier transform per time interval at the expense of introducing additional approximations.

Both attenuation and dispersion corrections are included in these implementations. The fastest approach for phase-only inverse-Q dispersion corrections is described in Robinson (1979) and Hargreaves and Calvert (1991) that involves a forward and inverse Fourier transform only.

All inverse Q filtering approaches based on equations 9, 10 and variants are, however, very versatile because they can handle dispersion and/or attenuation corrections based on whether the first and/or second exponent are incorporated into the algorithm. They are convenient in that no explicit knowledge is required of the propagating wavelet at any stage, contrary to the time-varying Wiener deconvolution. Also, these equations are formulated in terms of two-way traveltime t and require therefore no knowledge of the underlying velocity field.

They do require a sufficiently accurate estimate of the quality factor Q. Trantham (1994) provides some guidance on the desired accuracy for dispersion corrections. Estimation of attenuation parameters is reasonably straightforward for vertical seismic profile data (Hauge 1981; Tonn, 1991; Quan and Harris, 1997). Unfortunately, this is not necessarily true for its estimation from surface seismic data, although some robust methods have recently been developed (Reine et al., 2009, 2012a, 2012b).

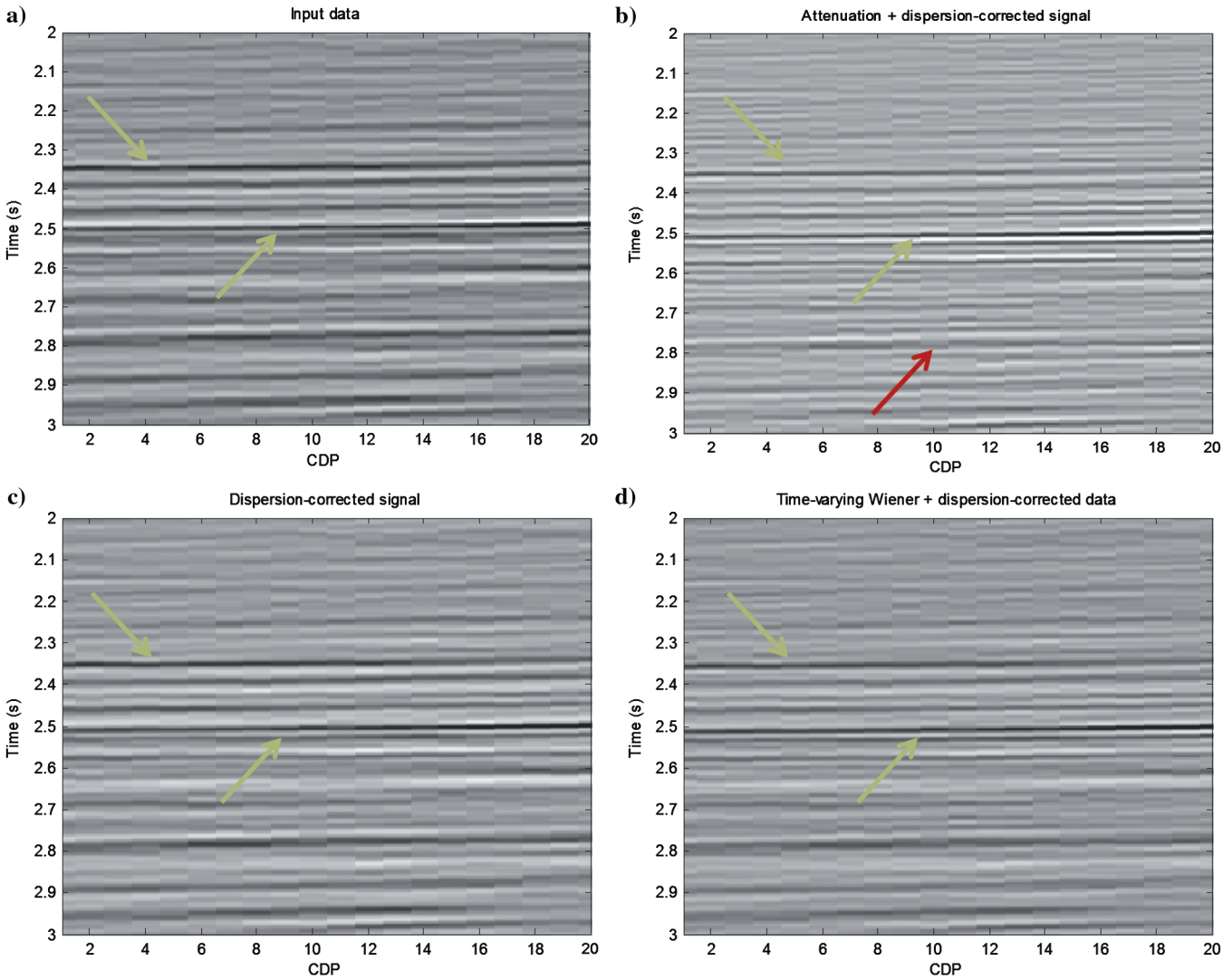

Figure 3. Data set 1. (a) Original data set. (b) Constrained amplitude-and-phase inverse Q filtering has compacted the major reflectors but several minor ones are now hidden by the noise. (c) Dispersion corrections using phase-only inverse Q filtering creates symmetric zero-phase wavelets without noise amplification. (d) Zero-phase time-varying Wiener deconvolution applied after phase-only inverse Q filtering boosts again the bandwidth and resolution but without significant noise amplification. The horizontal axis spans 250 m.

The described implementation assumes a constant Q value for all recorded traveltimes. This is a limitation of the implementation, not equation 9. Indeed, it is possible to extend such wavefield extrapolation-based methods to handle variations in attenuation using a layer-stripping approach by subdividing a single time step Δt into several ones for each constant-Q isochron (Hargreaves and Calvert, 1991; Wang, 2002). This is feasible in the described implementation as well but at the expense of computational efficiency.

A second disadvantage of expression 9 is that it implicitly assumes that all recorded data $u(t, t_0)$ are source signals and thus noiseless. Indeed, this is not necessarily problematic for dispersion corrections because no energy is boosted, conversely to attenuation corrections. In the latter case, expression 9 often reduces the overall S/N as seen in the examples (Figures 1–4). To prevent undue high-frequency noise amplification, it is industry practice to apply a high-cut or band-pass filter after inverse Q filtering.

The time-varying Wiener deconvolution relies on accurate estimation of the nonstationary propagating wavelet. Estimation of the changing amplitude spectrum via spectral averaging is straightforward and robust because only first- and second-order statistics are involved (van der Baan, 2008). Equating the measured amplitude spectra to those of the propagating wavelet does assume the underlying reflectivity series are white. Analysis of well logs has shown that reflectivity series tend to be blue instead of white, thus lacking low vertical wavenumbers (Walden and Hosken, 1985). This nonwhiteness is generally considered to be a second-order problem, unless the data are characterized by an unusual bandwidth, comprising, for example, five or more octaves. It can also be remedied easily if local well logs exist (Saggaf and Robinson, 2000).

Estimation of the time-varying phase spectrum is more challenging because only higher-order statistics retain phase information (Mendel, 1991). Unfortunately, estimation variances also increase with statistical order (Mendel, 1991). Van der Baan and Pham

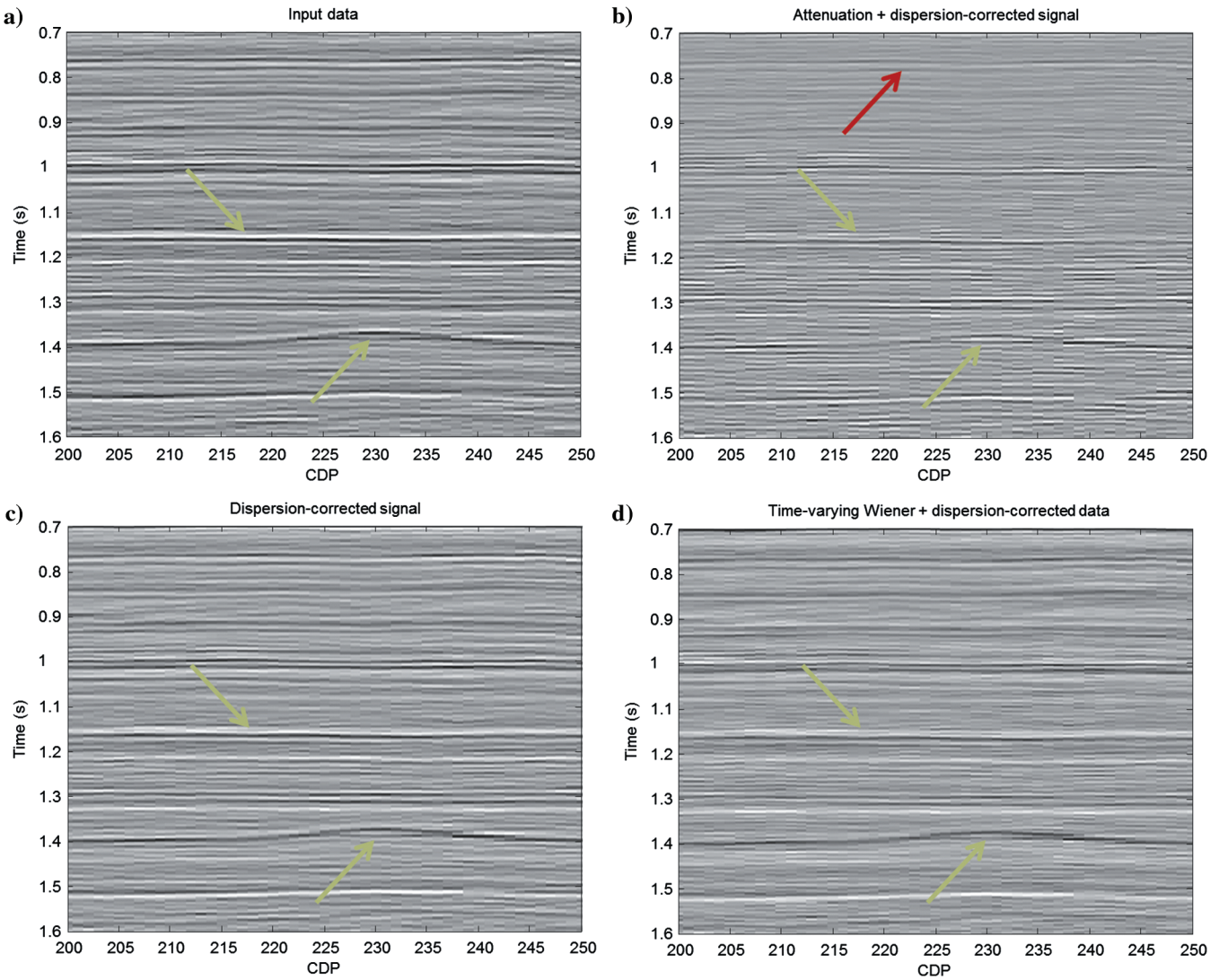

Figure 4. Data set 2. (a) Original data set. (b) Constrained amplitude-and-phase inverse Q filtering improves the resolution of several major reflectors but minor ones are lost in the noise. (c) Dispersion corrections using phase-only inverse Q filtering creates symmetric zero-phase wavelets without noise amplification. (d) Zero-phase time-varying Wiener deconvolution applied after phase-only inverse Q filtering boosts again the bandwidth and resolution but without significant noise amplification. The horizontal axis spans 750 m.

(2008) develop one method to estimate the frequency dependent phase spectrum of a stationary wavelet from noisy seismic data. An extension of this method to time-varying wavelets would greatly increase the number of degrees of freedom, rendering successful application even more challenging because estimation variances are also inversely proportional to the number of independent data points used (Mendel, 1991).

On the other hand, the number of degrees of freedom can be significantly decreased if one assumes that the wavelet has a frequency-dependent amplitude spectrum but a constant phase (Levy and Oldenburg, 1987; Longbottom et al., 1988; White, 1988). An extension to nonstationary wavelets is then possible (van der Baan, 2008; van der Baan and Fomel, 2009), but insufficient if dispersion corrections are required because the latter are frequency dependent by their very nature (equations 3 and 4).

This does not imply that statistical wavelet estimation cannot yield results similar to those obtained using other approaches, such as seismic-to-well ties. Edgar and van der Baan (2011) analyze three marine data sets and find a close similarity between both wavelet estimates, although the statistical wavelets tended to be simpler with less sidelobes (that is, less wiggles). Their work gives confidence in the reliability of statistical wavelet estimates as long as their underlying assumptions are honored.

Finally, there is significant overlap between the time-varying Wiener deconvolution and the Gabor deconvolution (Margrave et al., 2011). The latter technique also deconvolves an estimate of the nonstationary propagating wavelet from the seismic response. There are, however, a few important differences. First, the Gabor deconvolution is achieved by a simple spectral division in the frequency domain. A damping coefficient similar to the noise variance σ_n^2 (equation 15) is used to prevent division by zero. The Wiener deconvolution (equation 15) on the other hand, is based on a least-squares optimization framework to find an optimal trade-off between recovery of the reflectivity series and noise amplification (Berkhout, 1977).

Second, the Gabor deconvolution assumes the propagating wavelet is always minimum phase to circumvent the problem of phase estimation. The computation of a minimum-phase wavelet requires the calculation of the Hilbert transform, which is a precarious operation for short time series. Also there is no imminent reason why the propagating wavelet should be minimum phase unless the near-surface wavelet is already minimum due to acquisition or processing. On the other hand, if the propagating wavelet is indeed minimum phase and its amplitude spectrum has been accurately estimated at all times, the Gabor deconvolution can compensate for dispersion and attenuation without explicit knowledge of the quality factor Q. The described method of the time-varying Wiener deconvolution requires estimation of a nonstationary, nonminimum phase, albeit constant-phase, wavelet. This is feasible using the kurtosis-maximization framework developed in Levy and Oldenburg (1987), Longbottom et al. (1988), White (1988), van der Baan (2008), and van der Baan and Fomel (2009).

A final difference is that the time-varying Wiener deconvolution is explicitly formulated in terms of an estimated wavelet, equation 15. This has the advantage that the nonstationary wavelet can be inspected which may act as a more familiar quality-control tool than inspection of a nonstationary inverse filter (van der Baan, 2008).

CONCLUSIONS

Phase-only inverse Q filtering for dispersion correction of seismic data is inherently stable. It has the advantage over the time-varying Wiener deconvolution that no frequency-dependent, nonminimum phase, nonstationary propagating wavelet needs to be estimated. Phase-only inverse Q filtering is also a deterministic process that is repeatable and reversible.

Attenuation corrections, on the other hand, are best achieved using the time-varying Wiener deconvolution after estimation of the zero-phase equivalent of the nonstationary propagating wavelet. The explicit advantage of the time-varying Wiener deconvolution is that it balances noise amplification and resolution enhancement by whitening the signal bandwidth only within the wavelet passband.

Both dispersion and attenuation corrections enhance resolution. Superior results are thus achieved by first applying dispersion correction using phase-only inverse Q filtering, followed by pure attenuation corrections using the time-varying Wiener deconvolution.

ACKNOWLEDGMENTS

The author thanks Petrobakken and Shell for permission to use and show the real data examples, Chevron and Statoil for financial support of the project Blind Identification of Seismic Signals, and Anatoly Baumstein, Gary Margrave, and two anonymous reviewers for their comments and suggestions.

REFERENCES

Berkhout, A. J., 1977, Least-squares inverse filtering and wavelet deconvolution: Geophysics, **42**, 1369–1383, doi: 10.1190/1.1440798.
Bickel, S. H., and R. R. Natarajan, 1985, Plane-wave Q deconvolution: Geophysics, **50**, 1426–1439, doi: 10.1190/1.1442011.
Birdus, S., and A. Artyomov, 2011, Depth imaging with amplitude correction for localized absorption anomalies: The North-West Australian Shelf case study: 73rd Annual Conference and Exposition. EAGE, Extended Abstracts, E042.
Cavalca, M., I. Moore, L. Zhang, S. L. Ng, R. P. Fletcher, and M. P. Bayly, 2011, Ray-based tomography for Q estimation and Q compensation in complex media: 73rd Annual Conference and Exposition, EAGE, Extended Abstracts, E044.
Clarke, G. K. C., 1968, Time-varying deconvolution filters: Geophysics, **33**, 936–944, doi: 10.1190/1.1439987.
Duren, R. E., and E. C. Trantham, 1997, Sensitivity of the dispersion correction to Q error: Geophysics, **62**, 288–290, doi: 10.1190/1.1444129.
Edgar, J. A., and M. van der Baan, 2011, How reliable is statistical wavelet estimation?: Geophysics, **76**, no. 4, V59–V68, doi: 10.1190/1.3587220.
Ferber, R., 2005, A filter bank solution to absorption simulation and compensation: 75th Annual International Meeting, SEG, Expanded Abstracts, 2170–2172.
Futterman, W. I., 1962, Dispersive body waves: Journal of Geophysical Research, **67**, 5279–5291, doi: 10.1029/JZ067i013p05279.
Hargreaves, N. D., and A. J. Calvert, 1991, Inverse Q filtering by Fourier transform: Geophysics, **56**, 5119–527, doi: 10.1190/1.1443067.
Hauge, P., 1981, Measurements of attenuation from vertical seismic profiles: Geophysics, **46**, 1548–1558, doi: 10.1190/1.1441161.
Kjartansson, E., 1979, Constant-Q wave propagation and attenuation: Journal of Geophysical Research, **84**, 4737–4748, doi: 10.1029/JB084iB09p04737.
Levy, S., and D. W. Oldenburg, 1987, Automatic phase correction of common- midpoint stacked data: Geophysics, **52**, 51–59, doi: 10.1190/1.1442240.
Longbottom, J., A. T. Walden, and R. E. White, 1988, Principles and application of maximum kurtosis phase estimation: Geophysical Prospecting, **36**, 115–138, doi: 10.1111/gpr.1988.36.issue-2.
Margrave, G. F., M. P. Lamoureux, and D. C. Henley, 2011, Gabor deconvolution: Estimating reflectivity by nonstationary deconvolution of seismic data: Geophysics, **76**, no. 3, W15–W30, doi: 10.1190/1.3560167.
Mendel, J. M., 1991, Tutorial on higher-order statistics (spectra) in signal processing and system theory: Proceedings of the IEEE, **79**, 278–305, doi: 10.1109/5.75086.

Mittet, R., 2007, A simple design procedure for depth extrapolation operators that compensate for absorption and dispersion: Geophysics, **72**, no. 2, S105–S112, doi: 10.1190/1.2431637.

Quan, Y., and J. M. Harris, 1997, Seismic attenuation tomography using the frequency shift method: Geophysics, **62**, 895–905, doi: 10.1190/1.1444197.

Reine, C., R. Clark, and M. van der Baan, 2012a, Robust prestack Q-determination using surface seismic data: I — Method and synthetic examples: Geophysics, **77**, no. 1, R45–R56, doi: 10.1190/geo2011-0073.1.

Reine, C., R. Clark, and M. van der Baan, 2012b, Robust prestack Q-determination using surface seismic data: II — 3D case study: Geophysics, **77**, no. 1, B1–B10, doi: 10.1190/geo2011-0074.1.

Reine, C., M. van der Baan, and R. Clark, 2009, The robustness of seismic attenuation measurements using fixed- and variable-window time-frequency transforms: Geophysics, **74**, no. 2, WA123–WA135, doi: 10.1190/1.3043726.

Robinson, J. C., 1979, A technique for the continuous representation of dispersion in seismic data: Geophysics, **44**, 1106–1110, doi: 10.1190/1.1441011.

Saggaf, M. M., and E. A. Robinson, 2000, A unified framework for the deconvolution of traces of nonwhite reflectivity: Geophysics, **65**, 1660–1676, doi: 10.1190/1.1444854.

Schoenberger, M., 1974, Resolution comparison of minimum-phase and zero-phase signals: Geophysics, **39**, 826–833, doi: 10.1190/1.1440469.

Tonn, R., 1991, The determination of the seismic quality factor Q from VSP data: A comparison of different computational methods: Geophysical Prospecting, **39**, 1–27, doi: 10.1111/gpr.1991.39.issue-1.

Trantham, E. C., 1994, Controlled-phase acquisition and processing: 64th Annual International Meeting, SEG, Expanded Abstracts, 890–894.

van der Baan, M., 2008, Time-varying wavelet estimation and deconvolution by kurtosis maximization: Geophysics, **73**, no. 2, V11–V18, doi: 10.1190/1.2831936.

van der Baan, M., and S. Fomel, 2009, Nonstationary phase estimation using regularized local kurtosis maximization: Geophysics, **74**, no. 6, A75–A80, doi: 10.1190/1.3213533.

van der Baan, M., S. Fomel, and M. Perz, 2010, Nonstationary phase estimation: A tool for seismic interpretation?: The Leading Edge, **29**, 1020–1026, doi: 10.1190/1.3485762.

van der Baan, M., and D.-T. Pham, 2008, Robust wavelet estimation and blind deconvolution of noisy surface seismics: Geophysics, **73**, no. 5, V37–V46, doi: 10.1190/1.2965028.

Walden, A. T., and J. W. J. Hosken, 1985, An investigation of the spectral properties of primary reflection coefficients: Geophysical Prospecting, **33**, 400–435, doi: 10.1111/gpr.1985.33.issue-3.

Wang, R. J., 1969, The determination of optimum gate lengths for time-varying Wiener filtering: Geophysics, **34**, 683–695, doi: 10.1190/1.1440040.

Wang, Y., 2002, A stable and efficient approach of inverse Q filtering: Geophysics, **67**, 657–663, doi: 10.1190/1.1468627.

Wang, Y., 2006, Inverse Q-filter for seismic resolution enhancement: Geophysics, **71**, no. 3, V51–V60, doi: 10.1190/1.2192912.

White, R. E., 1988, Maximum kurtosis phase correction: Geophysical Journal International, **95**, 371–389, doi: 10.1111/gji.1988.95.issue-2.

Ziolkowski, A., J. R. Underhill, and R. G. K. Johnston, 1998, Wavelets, well ties, and the search for subtle stratigraphic traps: Geophysics, **63**, 297–313, doi: 10.1190/1.1444324.